A Model of aging for gas-filled cellular plastics
Bomberg, M. T.

National Research Council Canada   Conseil national de recherches Canada

Canada

**National Research
Council Canada**

**Conseil national
de recherches Canada**

Institute for
Research in
Construction

Institut de
recherche en
construction

A Model of Aging for Gas-Filled Cellular Plastics

by M. Bomberg

ANALYZED

NRCC 29770
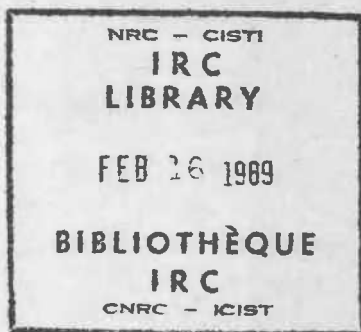
Canadä

ABSTRACT

During the service life of gas-filled cellular plastics (GFCP), air diffuses into the foam cells and the gaseous blowing agent diffuses out, each at a rate that depends on type of polymer and temperature. This process, which reduces the effectiveness of insulation, is known as aging.

This paper presents a model for calculating the thermal resistance of the GFCP slab as a function of time. It incorporates the effect of phase changes (condensation and evaporation) in the gaseous blowing agent and the use of material characteristics (diffusion coefficient) varying in the cross-section of the GFCP slab. The results are compared with measurements.

RÉSUMÉ

Pendant la durée de service des plastiques cellulaires emplis de gaz (PCEG), l'air se répand dans les cellules de mousse et l'agent porogène gazeux s'échappe par diffusion, chacun à un taux qui dépend du type de polymère et de la température. Ce processus, qui diminue l'efficacité de l'isolant, est connu sous le nom de "viellissement".

Ce document présente un modèle servant à calculer la résistance thermique du panneau de PCEG en fonction du temps. Il tient compte de l'effet des changements de phase (condensation et   ainsi que de l'utilisation des   nt dans la coupe de pann

A Model of Aging for
Gas-Filled Cellular Plastics

M. BOMBERG

National Research Council Canada
Institute for Research in Construction
Ottawa, Ontario

1. INTRODUCTION

A previous paper [1] introduced the necessity of integrating experiments and modelling in predicting long-term thermal resistance of gas-filled cellular plastics (GFCP). The present paper concentrates on the modelling aspect of integrated evaluation, reviewing the equations used in the model and the method of their solution. The results of calculations for one GFPC product are compared with measured values.

During the service life of GFCP insulation air components diffuse into the cells and CFC gas diffuses out, modifying the cell-gas composition. Moreover, a fraction of the CFC enters and saturates the polymer matrix, depending on the polymer type and temperature. The net effect is a gradual loss of thermal resistivity of the foam.

As the inward diffusion of nitrogen and oxygen is much faster than that of CFC outward, the aging process comprises two stages:

1. A thermal drift stage when composition of the cell gas changes at a significant rate, mainly by the influx of air
2. A plateau stage when air diffusion is almost complete and the

lower-rate efflux of CFC causes a very slow decrease in thermal resistivity with time

Norton [2] was the first to propose a model of isothermal, multi-component diffusion for calculating thermal resistance changes with time. This model, however,

1. Required knowledge of thermal resistance at the final stage of air-filled foam (information usually not available)
2. Approximated thermal conductivity of a gas mixture as linearly dependent on molar fraction of chlorofluorocarbon (CFC) gas
3. Did not relate to the material structure

Such drawbacks were partly eliminated in a subsequent model developed at MIT [3–6]. The MIT model assumed the following:

1. Heat transfer by radiation is separate from and independent of heat conduction.
2. Radiative heat transfer is described by the Rosselund approximation [7].
3. Solid phase conduction depends on material porosity, conduction of the polymer film and distribution of polymer between material in the cell-walls (membranes or windows) and material deposited at interstices of cells (struts).
4. Conduction of a gas mixture may be calculated when viscosity, thermal conductivity, and the relative amounts of each component are known.

Although an improvement on Norton's linear approximation, the MIT model failed to observe that the composition of cell-gas and therefore its thermal conductivity are strongly affected by the phase change of CFC (condensation and evaporation). Moreover, heat release and extraction involved in condensation and the evaporation process may affect the apparent thermal conductivity of the foam.

The present paper presents a model of aging of GFCP incorporating the effect of CFC condensation and evaporation. Its application (as that of other models) is, however, limited by the lack of proper input parameters (initial CFC pressure and diffusion coefficients) [1]. An attempt to determine these properties is therefore included in the methodology discussed.

2. MODEL OF AGING FOR GAS-FILLED CELLULAR PLASTICS

The objective is to calculate, at any given time, the heat flux through a foam slab exposed to a specific temperature difference. To perform

this calculation, time is divided into a number of steps and the slab is divided into a number of layers. For each time and space step four separate equations are evolved that calculate temperature and partial pressures of oxygen, nitrogen, and CFC, all necessary in determining the composition of the cell-gas.

The ability to calculate the cell-gas composition at selected locations in the GFCP product as a function of time is the most important aspect of the model. As other components of heat transfer (solid phase conduction, radiation, interaction between radiation and solid phase conduction) may be assumed constant, the addition of the variable contribution of cell-gas conduction gives the total conduction for a given layer.

Unless, however, phase changes for CFC gas have been taken into consideration, the cell-gas composition is not correct. Phase change of CFC (evaporation and condensation) affects the calculation of heat flux in two ways:

1. It modifies the composition of the cell-gas, thus directly affecting its thermal conductivity.
2. It extracts or releases heat (during phase change) thus affecting the heat flux through the foam slab.

At any given time step the model calculates

1. Temperature
2. Partial pressures of oxygen, nitrogen, and CFC
3. Saturation partial pressure of CFC and mass of CFC condensing or evaporating to maintain equilibrium
4. Thermal conductivity of the foam
5. Heat flux caused by evaporation, diffusion, and condensation of CFC

Several simplifying assumptions are made. The most important is, perhaps, the assumption that boundary conditions and material properties remain unchanged during a time step. Moreover, all material properties used in a given time step are those calculated in the previous time step. This simplification is necessary because all the (discussed) heat and mass transfer phenomena are interrelated. A change in temperature may cause a change in the partial pressure of any gas or a change in equilibrium between condensed and gaseous CFC. A change in partial pressures affects thermal conductivity of cell-gas and alters the heat flux. The assumption therefore simplifies the calculations but imposes limitations on the time steps used.

Another simplification incorporated in the model is the assumption of uncoupled flow phenomena. For all points between boundaries, each

energy or mass conservation equation is separate from the other equations. To account for the coupling between heat and mass transfer, the heat flux caused by mass transfer is calculated in an approximate manner for each time step. This simplified calculation is permissible because, in applying later calculations over a wide range of temperatures (140–320 K), the maximum mass transfer contribution to heat transfer was found to be less than 6% of the total heat transfer in PUR slabs.

2.1 Temperature Distribution

A one-dimensional energy conservation equation can be expressed in a finite difference form [4] as:

$$C_p \varrho \frac{T_i^{n+1} - T_i^n}{\Delta t} = \frac{\lambda_i^n}{\Delta x^2} \left[\frac{1}{2} (T_{i-1}^{n+1} - 2T_i^{n+1} + T_{i+1}^{n+1}) + \frac{1}{2} (T_{i-1}^n - 2T_i^n + T_{i+1}^n) \right]$$

(1)

where indices n and i relate to steps in time and space (layer number), respectively; T is temperature (K); Δx is the distance between two adjacent positions in space (space step) (m); Δt is the time step used for calculations (s); C_p is the specific heat of the foam as the whole (J/kg·K); ϱ is density (kg/m³); and λ is the thermal conductivity of the foam (W/m·K). Equation (1) gives the temperature at each node at time $n + 1$, using the values of λ and T from the previous time step.

2.2 Gas Pressure Distribution

The one-dimensional mass conservation equations are written in a finite difference form and relate to the partial pressure of each component. The equations for partial pressure of oxygen, nitrogen, and CFC take the form:

$$\frac{P_i^{n+1} - P_i^n}{\Delta t} = \frac{D_i^n}{\Delta x^2} \left[\frac{1}{2} (P_{i-1}^{n+1} - 2P_i^{n+1} + P_{i+1}^{n+1}) + \frac{1}{2} (P_{i-1}^n - 2P_i^n + P_{i+1}^n) \right] \quad (2)$$

where indices n and i relate to steps in time and space, respectively. P is the partial pressure of a gas (Pa); D is the effective diffusivity of the foam (cm²/s), Δx is the distance between two adjacent position in space (space step) and Δt is the time step used for calculations.

The effective diffusion coefficient for each layer is assumed to be constant and independent of concentration for a given gas. Moreover, to simplify calculations [1], one may assume a constant ratio between oxygen and nitrogen diffusion. In this work the effective diffusion coefficient for oxygen is assumed to be six times higher than the nitrogen diffusion coefficient [4,8,9].

The model allows the effective diffusion coefficients to vary in the cross-section of the foam. Nitrogen diffusion was estimated for each surface layer and for the middle of the material. The calculation assumed:

1. Effective nitrogen diffusion coefficient for the middle (i.e., one half material thickness) may be taken as the average of two estimates of core material; a linear transition is then applied between this level and those at each surface (Figure 1).
2. The effective CFC diffusion coefficient is assumed to vary across the material in the same manner as the effective nitrogen coefficient.

Equation (2) gives the pressure changes caused by diffusion through the foam. For CFC gas, however, one must also consider another phenomenon affecting pressure changes: condensation or evaporation of CFC. Thus, CFC pressure calculated with Equation (2) will be corrected for phase changes.

2.3 Correcting Partial Pressure for Condensation of CFC

If the partial pressure of CFC exceeds the vapour-liquid equilibrium pressure for a given temperature, condensation will occur. The equi-
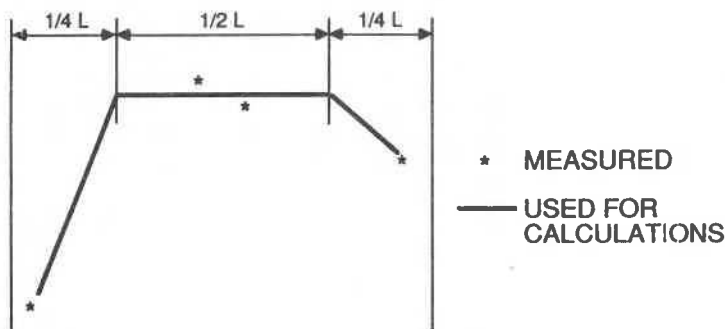

Figure 1. Measured and assumed variation of effective diffusion coefficients across slab thickness.

librium pressure of CFC is calculated from an appropriate form of Clapeyron's equation [10]

$$P_s(T) = 101325.0 \exp\left(C_0 \frac{T - T_b}{T_b} \right) \tag{3}$$

where p_s is the equilibrium partial pressure of CFC in Pa; T is the temperature in K; T_b is the normal boiling temperature (at one atmosphere); and $C_0 = 10.0$. Compared with the process of diffusion through the polymeric material of cell-walls, the process of phase change may be considered instantaneous. Thus, the model assumes that vapour pressure above the condensed CFC is always in equilibrium. If the actual CFC pressure calculated from Equation (2) exceeds the equilibrium pressure, CFC will condense until equilibrium pressure is reached. Conversely, if there is liquid CFC and the CFC partial pressure is below that calculated from Equation (3), an evaporation of CFC will continue until the actual pressure reaches an equilibrium pressure.

2.4 Thermal Conductivity of Foam

Thermal conductivity of the foam is calculated from the equation introduced by Schuetz and Glicksman [3]:

$$\lambda = \lambda_g + 0.8 \left(\frac{2}{3} - \frac{f_s}{3} \right)(1 - \delta)\lambda_p + \frac{16\sigma}{3K\varrho} T_m^3 \tag{4}$$

where λ_g is thermal conductivity of a gas mixture (W/m·K); f_s is the fraction of struts in the foam; δ is the foam porosity; σ is the Steffan-Boltzman constant 5.67×10^{-8} W/(m²K⁴); K is the mass extinction coefficient (m²/kg); T_m is the mean temperature of the foam layer (K).

Some of the parameters used in Equation (4) were modified, namely:

1. The coefficient of thermal conductivity of a gas mixture, λ_g, is calculated from the equations developed by Mason and Saxena [11] for a mixture of polyatomic gases;

$$\lambda_{mix} = \sum_{i=1}^{n} \frac{\lambda_i}{\displaystyle\sum_{\substack{k=1 \\ k \neq i}}^{n} G_{ik} \frac{f_k}{f_i}} \tag{5}$$

where

$$G_{ik} = 0.3765 \, [1 + (M_i/M_k)]^{-1/2} \, [1 + (\lambda_i^0/\lambda_k^0)^{1/2} \, (M_i/M_k)^{1/4}]^2$$
$$(\lambda_i^0/\lambda_k^0) = (\eta_i M_k/\eta_k M_i)$$

f_i = mole fraction of ith component

M_i = molecular weight of ith component

λ_i, η_i = thermal conductivity and dynamic viscosity of ith component

Properties of each gas such as thermal conductivity and viscosity, taken from handbooks and general property tables [12,13] were expressed as linear functions of temperature. Two temperature ranges were used: construction applications (240–340 K), cryogenic applications (170–240 K).

2. Instead of the extinction coefficient, a mass extinction coefficient (i.e., the former divided by density of the foam) is used. It does not include the effects of porosity variation and provides better means of polymer characterization. Moreover, if a broad range of temperatures is examined, the mass extinction coefficient is approximated by linear temperature dependence [14]:

$$K = K_0 + C(T - 273.2) \tag{6}$$

where K_0 is the extinction coefficient at $0°C$ and C is the temperature dependence of the extinction coefficient.

Having calculated thermal conductivity of each of n layers, λ_i, one may calculate thermal resistance of the slab

$$R_s = \sum_{i=1}^{n} \frac{\Delta x_i}{\lambda_i} \tag{7}$$

where Δx_i is the thickness of each layer. If a particular temperature difference, ΔT, is imposed on the slab, the heat flux under steady-state conditions becomes

$$q = \frac{\Delta T}{R_s} \tag{8}$$

The heat flux calculated from Equation (8) does not include the effect of mass transfer.

2.5 Heat Flux Approximation for Evaporation, Diffusion, and Condensation of CFC

In addition to affecting thermal conductivity of cell-gas by modifying its composition, the phase change of CFC affects heat flux by extracting or releasing heat. An appropriate method of calculating a limiting case of heat flux due to latent heat release or extraction is introduced below. This heat flux is assumed to be the product of two components:

1. Maximum amount of latent heat transfer under the effect of actual boundary conditions, assuming that all CFC is on the hot side, diffused, and condensed on the cold side of each pore
2. Reduction of the efficiency of the liquid flow rate to return the condensed CFC to the hot side of the cell if only a part of CFC is condensed

Component 1: A maximum heat flux caused by diffusion of CFC through the cell gas, q_m^h, under conditions imposed by the boundary surfaces is calculated. It is assumed that air diffusion in the foam is already complete and that the whole mass of CFC evaporates, diffuses, and condenses, and then is transferred in the opposite direction by the liquid flow. It may be calculated from the following equation:

$$q_m^h = H_{ev} D_f^a \frac{1}{RL}\left(\frac{P_1}{T_1} - \frac{P_2}{T_2}\right) \tag{9}$$

where H_{ev} is the latent heat of CFC evaporation, D_f^a is the coefficient of CFC diffusion in air, R is the gas constant, L is the thickness of the slab, P_1 and P_2 are the saturation partial pressures at respective surfaces, and T_1 and T_2 are temperatures.

Component 2: This component describes the reduction of the efficiency of the liquid flow rate that returns condensed CFC to the hot side of the cell in relation to degree of saturation with liquid CFC. It may be calculated as follows:

$$C_2 = S_f^3 \tag{10}$$

where S_f is the degree of saturation with liquid CFC. This degree of saturation is assumed to be 1 when all fluorocarbon initially introduced to the foam is condensed. Equation (10) is derived from study of the relative permeability of the wetting phase as a function of degree of saturation [15–17].

The heat flux caused by evaporation, diffusion, and condensation of CFC may be calculated as:

$$q_m = H_{ev}D_f^e\text{grad}\left(\frac{p}{RT}\right)S_f^3 \tag{11}$$

Thus heat flux caused by evaporation, diffusion, and condensation can be calculated from Equation (11) and added to the heat flux calculated from Equation (8). This aggregate heat flux may then be used to compare results of calculations with actual measurements.

3. METHOD

3.1 Input: Material Characteristics and Initial and Boundary Conditions

To solve a set of differential equations such as Equation (1) and Equation (2) one must define boundary and initial conditions. While the boundary conditions (temperature and pressure of oxygen, nitrogen, and CFC in the environment) are known, this is not the case for the initial conditions of cell-gas composition.

CFC partial pressure, equal to approximately one atmosphere during the foaming process, is reduced owing to two phenomena:

1. Foam cools from the high temperature caused by exothermic reaction.
2. Part of CFC gas enters and saturates the polymer matrix.

As has been indicated [1], variability in the CFC solubility of different polymers coupled with large differences in the initial CFC pressure caused by cooling of foam makes it necessary to determine initial partial CFC pressure for each GFCP tested.

Equation (2) requires values for effective nitrogen and CFC diffusion coefficients. One possible method of determination is as follows. Several thin layers 40–80 mean cell-diameters thick are cut from different locations in the cross-section of the foam and placed in a Heat Flow Meter (HFM) apparatus immediately after slicing. Their thermal resistivity is continuously recorded over a 10- to 14-day period. The layers are then stored in the laboratory and periodically tested to determine the plateau stage of the R-value. Testing continues at less frequent intervals for several months. Thermal resistance changes in these thin specimens and the model of aging provide the effective diffusion coefficients. Diffusion of air components is calculated from the first stage of aging

(thermal drift) and diffusion of CFC is calculated from the second stage (plateau stage).

Calculation of the effective diffusion coefficients is as precise as the measurement of changes in the thermal resistivity of the specimen will permit. No additional assumptions are introduced. All three gas transfer processes are calculated under temperatures and temperature gradients used during the laboratory measurement of thermal resistivity. The calculations are performed for small steps in time and space (space increments do not exceed usually ten cell layers). For example, in calculating oxygen and nitrogen coefficients one assumes a specific value of CFC diffusion coefficient. If the difference between assumed and estimated (from another experiment) CFC diffusion coefficients affects the results of the first calculation, the calculation of nitrogen and oxygen diffusion is repeated, using a modified value of CFC diffusion.

While effective diffusion coefficients may be estimated with a high degree of confidence, this is not possible for initial CFC pressure in the GFCP. It is the most questionable element of the input data. In the present work initial pressure of CFC was estimated by two methods: chemical analyses and thermal conductivity measurements. The chemical analysis involved determining chlorine content twice: on undisturbed foam, and after rushing the foam and off-gasing the polymer powder (using a few hours' exposure to both vacuum and increase temperature). Assuming limited losses of CFC (either none or a known amount of chlorine included as the fire retardant agent), the fraction of gaseous CFC was calculated and used in the estimate of the initial CFC pressure. Large scatter of experimental results, uncertainty in content of chlorine in the added fire retardants, possible loss of CFC from surfaces of specimens caused low reliability of the chemical analysis. This method was used only for control purposes.

Initial CFC pressure was primarily estimated from the measured thermal resistivity at the end of thermal drift—beginning of the plateau aging stage. If other components of thermal conductivity (e.g., radiation and solid conduction) are known, one may estimate the molar fraction of a CFC gas in the cell-gas using the difference between them and the measured total conductivity of the foam. If there is only one type of CFC and if pressure of nitrogen and oxygen can be assumed equal to the atmospheric pressure (thin material layer at the beginning of plateau region), then one may estimate the "projected initial" CFC pressure.

Other input material characteristics are:

1. The extinction coefficient, determined by optical methods [2].

2. Fraction of struts and polymer thermal conductivity coefficient, either determined from a microscopic examination or estimated from the literature.

3.2 Method of Solving Equations

Analytic solutions exist for a number of simple isothermal cases. To permit calculations in more complex cases, e.g., involving phase change of CFC, one must use a numeric solution. As the transport coefficients in Equations (1) and (2) are non-linear, use of an average temperature for each layer may cause errors in the calculated pressures of oxygen, nitrogen, and CFC. To establish the magnitude of the errors, a comparison of the analytic and numeric solutions was made for a 40-mm thick, polyurethane slab aged at constant ambient temperature. As the analytic solution of Crank [18] is valid for long-term diffusion only, the discrepancy expected in the initial period of diffusion will not be analysed. The numeric calculations were performed by changing both the number of layers and the locations of the nodes, which were placed either in the centre of each layer or at the interface of two adjacent layers.

Equations (1) and (2) used a central difference formula, a version of the finite difference method of Ostrogorsky and Glicksmann [4], and
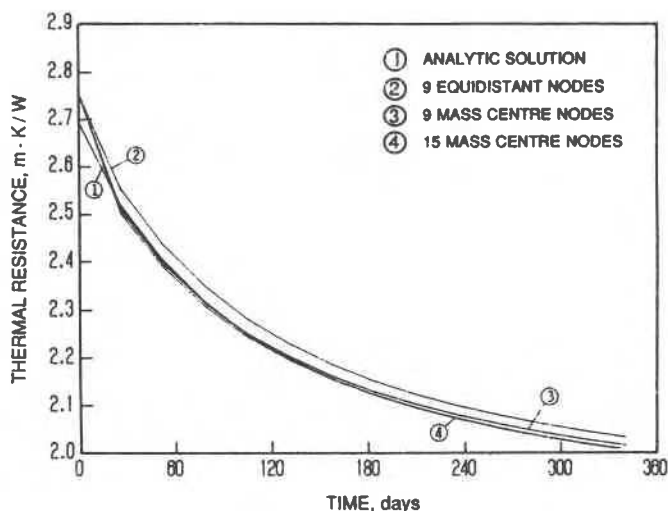

Figure 2. Comparison of analytic solution of Crank [18] with numerical solutions for 9 and 15 layers. Nodes placed at intersections (equidistant) or in the centre of each layer.

M. BOMBERG

Table 1. Density and initial thermal resistivity
(inverse of conductivity coefficient)
in 11 tests of selected polyisocyanurate (PIR) product.

Test code	Density kg/m³	Thermal resistivity, m·K/W
392-45	36.9	52.0
392-46	37.1	51.6
392-49	—	52.6
392-55	37.0	51.8
392-56	37.1	52.4
392-68	37.1	51.7
392-69	37.2	52.6
392-125	36.8	50.9
392-128	36.9	51.2
392-131	—	52.7
392-133	—	51.8
mean value		52.1
st. deviation		1.1%

were solved with an implicit scheme by the matrix inversion technique used by Kumaran and Mitalas [19].

Figure 2 illustrates that a large number of nodal points are necessary if the numeric solution is to agree with the analytic solution. Either fifteen layers with points at the intersections, or nine layers with points at the centre of each layer were found to be necessary. These calculations were also performed with different time steps to ensure that the choice of time step did not affect precision.

4. COMPARISON OF MEASURED AND CALCULATED THERMAL RESISTANCE

4.1 Input Data

Material characteristics of a selected polyisocyanurate (PIR) foam were measured at NRCC. This material was selected because of its small spatial variability as shown in Table 1, displaying initial thermal resistivity values of different specimens taken from the same batch. Measurements of attenuation of infrared radiation versus thickness of material gave a mass extinction coefficient of 42 m²/kg.

Thermal resistance of a 6-mm thick core layer of PIR at an initial stage of aging was used to estimate the effective nitrogen diffusion
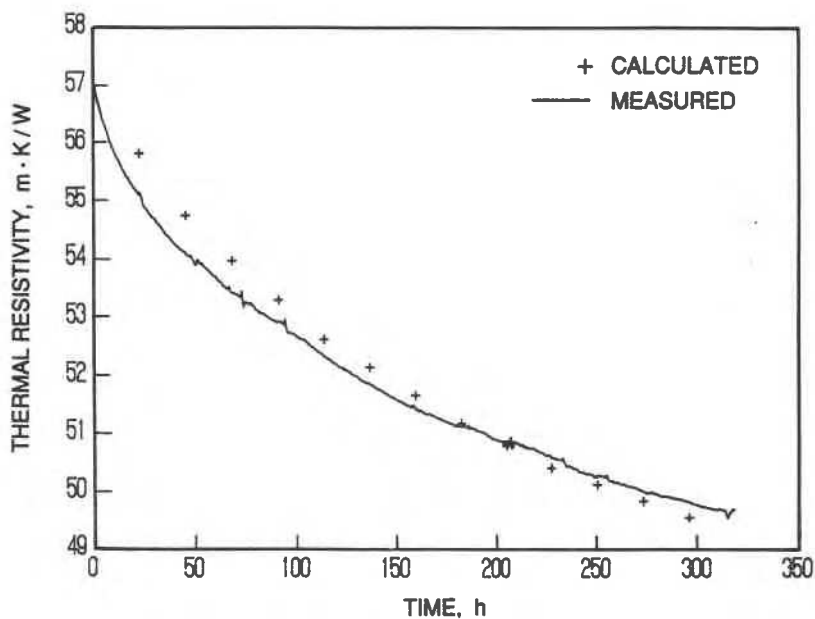
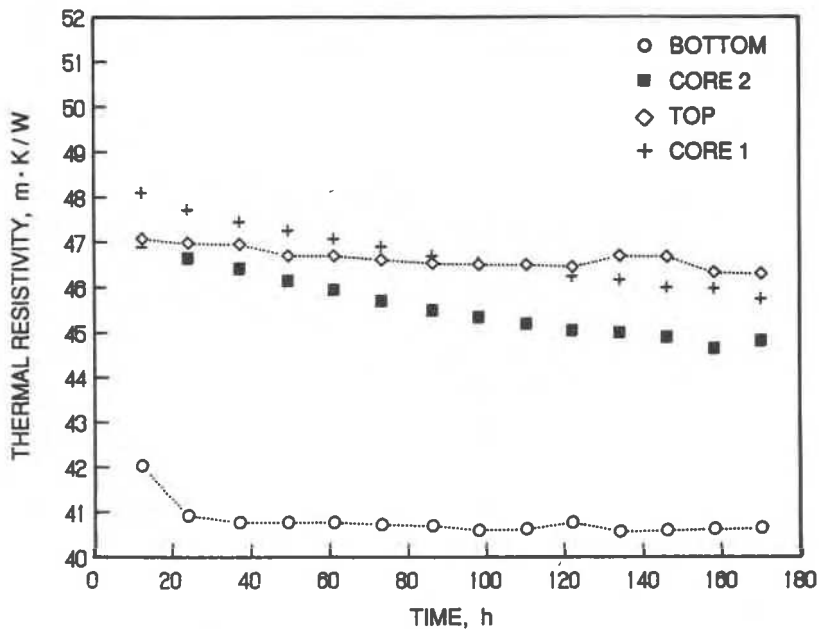**Figure 3.** Aging of 6-mm core layer of PIR at 10°C.

Figure 4. Aging of 6-mm layers cut from year-old PIR. Both storage and laboratory aging at 24°C.

coefficient, at the same time assuming a value of CFC diffusion coefficient from the literature [4,5]. A number of calculations were performed with different values of nitrogen diffusion coefficient, and the calculation giving the thermal resistivity curve closest to the measured one was selected. Figure 3 shows thermal resistivity measured at a mean temperature of 10°C over a period of 13 days and calculations performed with nitrogen diffusion coefficient of 0.2×10^{-7} cm²/s. The effective nitrogen diffusion coefficient was then adjusted to 60°C (temperature at which the long-term laboratory aging was performed).

Thermal resistance measurements were repeated on the same batch of PIR product one year later. This time a number of thin slices were cut from the centre of the board and from the layers adjacent to the board surface. Three or four slices were placed together in a stack and measured simultaneously in the HFM apparatus. Figure 4 shows the results of thermal resistivity measurements performed on four slices at a mean temperature of 24°C. These indicate unexpected and significant variability in the cross-section of the slab. As the specimens were cut from approximately 15 month old foam, the material layers exposed to air were expected to be at the plateau stage. Indeed, one of the surfaces (denoted as bottom) does show thermal resistivity at the plateau stage (41–42 m·K/W), but the other surface layer maintained a high
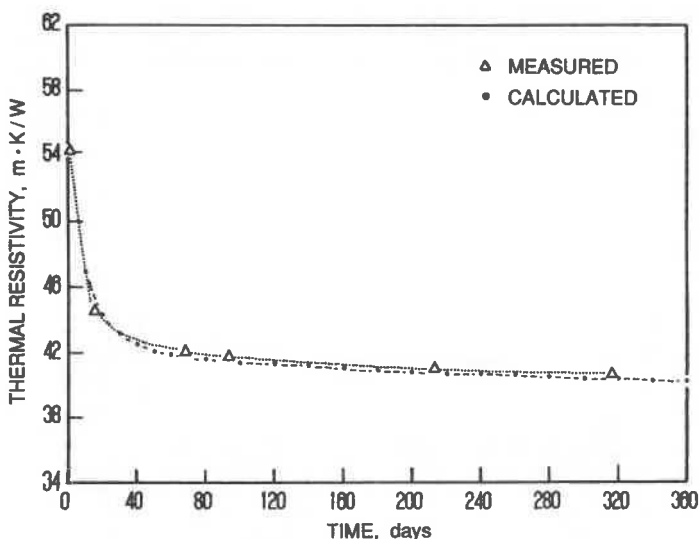

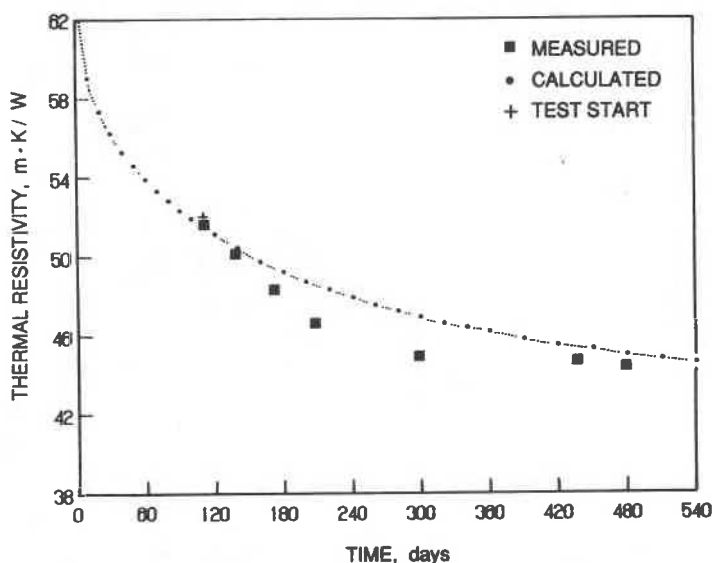**Figure 5.** Aging of 6-mm core layer of PIR at 60°C.

Figure 6. Measurements and calculations of full-thickness aging of PIR at 60°C.

thermal resistivity. It is evident that this top layer has a much higher resistance to gas diffusion than the bottom layer.

Comparing calculations to the measurements shown in Figure 4, the effective nitrogen diffusion coefficients were estimated as 0.3×10^{-6} cm²/s and 0.15×10^{-7} cm²/s for respective surfaces. (Nitrogen diffusion coefficient was estimated at 0.2×10^{-7} cm²/s for the core material.) The literature [4,5,8,18,20] also reports large variations in nitrogen diffusion determined on different PUR specimens.

Figure 5 shows thermal resistivity measured and calculated at 60°C. (A number of calculations were performed with different values of CFG diffusion coefficient and the calculation giving thermal resistivity curve closest to that measured was selected.) Effective CFC diffusion for the core of the foam was estimated at 0.1×10^{-8} cm²/s.

4.2 Thermal Resistance of PIR as a Function of Time

Having determined the material characteristics required as input, the output of the model (thermal resistance of the full board as a function of time) was compared with measured values. The period of material aging prior to testing must first be estimated. From the initial conditions and the diffusion coefficients of the PIR foam (Section 4.1), it

was calculated (using the model) that it takes 110 days at warehouse conditions to reach a thermal resistivity of 51.6 m·K/W, which was determined on the first day of the laboratory measurements. A vertical line at 110 days divides the period of initial aging from measurements performed in the laboratory (Figure 6). The largest difference between calculated and measured thermal resistivity is 4%, which is acceptable for the intended use of the model.

4.3 Thermal Resistance of PUR as a Function of Temperature

The model permits calculation of thermal resistance as a function of temperature. This is an important feature, particularly when long-term thermal resistance of GFCP is to be determined at different temperatures. While excellent data on the effect of temperature on thermal conductivity of GFCP exists, lack of characterization of the materials prohibited a direct calculation with the model. Another approach was used.

Thermal conductivity as a function of specimen mean temperature was measured at the National Bureau of Standards (NBS) by Sparks and Arvidson [21] and at the Padova University by Bigolaro et al. [22] on 32 kg/m³ aged polyurethane foam. Assuming that both materials reached the plateau stage, and taking one of the material characteristics from the literature (e.g., Oak Ridge National Laboratory communication, May 1986), a mass extinction coefficient of 55 m²/kg was taken for the NBS material. Performing calculations with different values of initial CFC concentrations, a CFC concentration was selected for which the R-value agreed with the measured R-value at 24°C. The question remains, however, whether a model calculation of R-value for other temperatures will be corroborated by measurements.

Figure 7 shows the thermal conductivity of the material tested at NBS calculated in two ways: (1) with a constant mass extinction coefficient $K_0 = 55$ m²/kg, and (2) with a linearly temperature-dependent mass extinction coefficient identical to that determined for air-filled polystyrene [$K_0 = 55$ m²/kg and $C = 0.27$ m²/kg °C, Equation (6)]. In both cases, Figure 7 shows acceptable agreement between calculated and measured values of thermal conductivity as a function of temperature.

For the material tested at Padova University (Figure 8), CFC pressure was assumed to be 50 kPa (10% less than that calculated for the NBS material). Inserting this value into the model to match a measured thermal resistivity at 24°C, the mass extinction coefficient was 28 m²/kg. Agreement in Figure 8 is also acceptable.
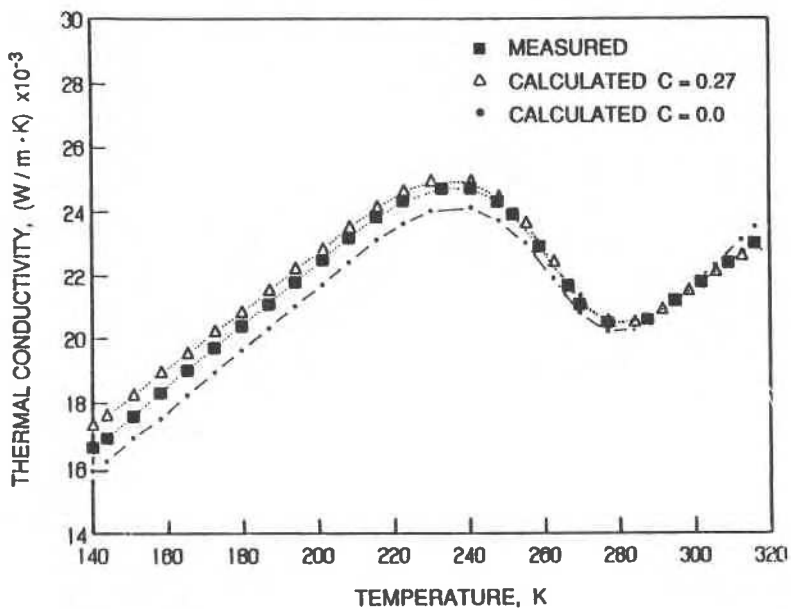
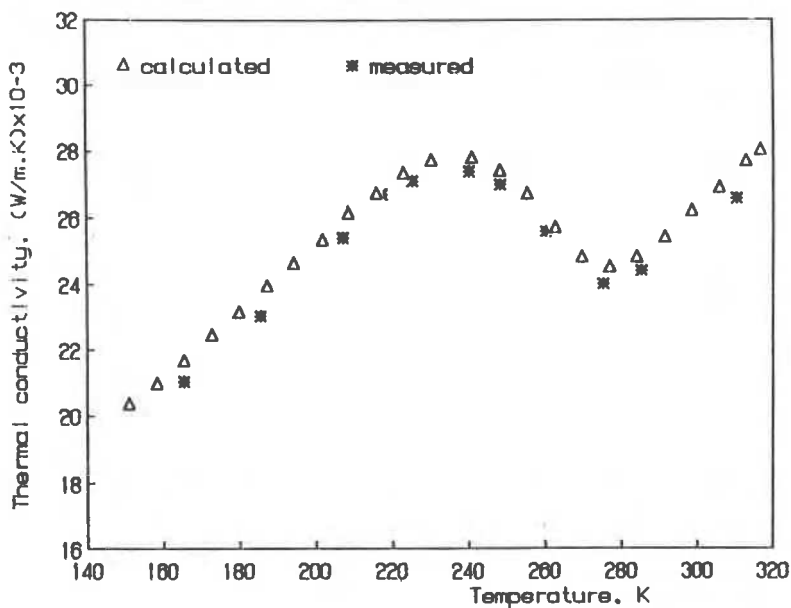**Figure 7.** Calculated thermal conductivity of PUR measured at NBS [21].

Figure 8. Calculated thermal conductivity of PUR measured at Padova University [22].

343

5. DISCUSSION

To calculate the thermal resistance of a product one must select representative effective diffusion coefficients. This issue requires more detailed discussion.

A difference in the level of thermal resistivity and rate of aging for specimens cut from different locations in the material cross-section are important (Figure 3). Table 2 shows thermal resistivity values using two approaches:

1. Disregarding spatial variability of the material and using constant diffusion coefficient of the core (D core)
2. Including the variation of the diffusion

Agreement of experimental results from the laboratory and calculations based on variable D is acceptable. For the calculation based on constant D, i.e., the core diffusion alone, agreement is not that good. Thus, if the diffusion coefficient is determined correctly, calculated and measured thermal resistivity values show better agreement.

Figure 4 shows significant variability in thermal resistivity of the foam layers. Although similar variability has been observed in sprayed PUR specimens such variability has not been observed in the PUR boards. It is important to emphasize that the results shown in Figure 4 relate only to a specific batch of the GFCP products.

Much more work must be done to establish the usefulness of the model. It should include improvement in methods of determining the material characteristics needed as input to the model, experiments with aging of other types of GFCP with either CFC or HCFC captive blowing agents (particularly if more than one is used), the statistical significance of various elements of product batch, board and cross-

Table 2. Thermal resistivity of PIR aged at 60°C according to calculations and measurement.

Time lapse	Measured	Calculated with diffusion coeff.	
		Varying across slab	Constant (core)
0	51.6	51.6	51.6
28	50.1	50.4	50.7
188	44.9	46.9	47.7
368	44.4	45.0	46.0
516	43.4	44.1	45.0

sectional variability. The thrust of this paper is simply to report the concept and to point out the key elements of future research.

6. CONCLUSIONS

A model developed to calculate changes in thermal resistance of GFCP slab as a function of time and temperature incorporates the effect of phase changes (condensation and evaporation) within the CFC and use of diffusion coefficients varying in the cross-section of the GFF slab.

The model has been used to calculate aging of PIR foam for which material characteristics and laboratory aging had been determined in the NRCC laboratory. As well, calculations were performed for PUR tested at NBS or Padova University, for which material characteristics were partly assumed and partly calculated when applying the model to the measured thermal resistance.

The following conclusions can be drawn from this work:

1. Thermal conductivity as a function of specimen mean temperature, calculated from the model, agrees well with the thermal conductivity of CFC-11 blown PUR boards measured by NBS [21] or Padova University [22] over cryogenic to ambient temperatures.
2. Acceptable agreement was obtained for thermal conductivity as a function of time when the effective diffusion coefficients of PIR board were carefully estimated. Selection of the effective diffusion coefficients, however, requires further investigation.
3. Comparison of calculated and measured thermal conductivity in relation to either temperature or time for PUR/PIR products indicates that this model may become a good complement to experimental evaluation of aging.

ACKNOWLEDGEMENTS

NRCC, for determination of the extinction coefficient of PUR and PIR foams.

In addition, and most importantly, two researchers from industry are to be thanked for their interest and encouragement during this work: Dr. Keith Linger, Fiberglas Canada Inc., and Dr. Sunil Vidarthi, Building Products of Canada.

REFERENCES

1. Bomberg, M. and D. A. Brandreth. "Evaluation of Long-Term Thermal Resistance of Gas-Filled Foams—A State-of-the-Art," ASTM Conference: Insulation Materials, Testing and Applications, Bal Harbour, to be published as STP of ASTM (Dec. 6–9, 1987).
2. Norton, F. J. *J. of Cellular Plastics,* pp. 23–37 (Jan. 1967).
3. Schuetz, M. A. and L. R. Glicksman. "A Basic Study of Heat Transfer Through Foam Insulation," *6th Int. Polyurethane Conference,* San Diego, CA., pp. 341–347 (1983); also *Advances of Foam Aging, Vol. 1.* D. A. Brandreth (ed.), Yorklyn, CAISSA editions (1986).
4. Ostrogorsky, A. G. and L. R. Glicksman. *Aging of Polyurethane Foams, the Influence of Gas Diffusion on Thermal Conductivity.* ORNL/SUB/84-9009/2, pp. 1–98 (1986).
5. Glicksman, L. R., A. G. Ostrogorsky and S. Chiapetta. *Effective Conductivity of Aging Polyurethane Foam.* ORNL/SUB/84-9009/1, pp. 1–56 (1986).
6. Reitz, D. W. "Heat Transfer and Aging of Closed-Cell Foam Insulation," *Advances in Foam Aging, Vol. 1.* D. A. Brandreth (ed.), Yorklyn, DE:CAISSA editions, pp. 110–130 (1986).
7. Siegel, R. and J. R. Howell. *Thermal Radiation Heat Transfer.* McGraw-Hill Book Co. (1972).
8. Brandreth, D. A. and H. G. Ingersoll. *European J. of Cellular Plastics,* 3:134–143 (1980); also *Advances in Foam Aging, Vol. 1.* D. A. Brandreth (ed.), Yorklyn, CAISSA editions (1986).
9. Norton, F. J. *J. of Cellular Plastics,* pp. 200–318 (Sept./Oct. 1982).
10. McGlashan, M. L. *Chemical Thermodynamics.* London:Academic Press Inc., p. 128 (1979).
11. Mason, E. A. and S. C. Saxena. *Physics of Fluids, Vol. 1.* p. 361 (1958).
12. *Handbook of Chemistry and Physics. 38th ed.* Chemical Rubber Publ. Co. (1956).
13. *"Freon" Fluorocarbons, Properties and Applications,* Bulletin G-1 DuPont.
14. Reiss, H. and B. Ziegenbein. "Temperature-Dependent Extinction Coefficient and Solid Thermal Conductivities of Glass Fibre Insulations," *Thermal Conductivity 18.* Plenum Press, pp. 412–424 (1985).
15. Irmay, S. *Trans. Amer. Geophys. Un.,* 35(3):463–467 (1954).
16. Brooks, R. H. and A. T. Corey. *J. Irrig. Drain.,* Div. Am. Soc. Civ. Engrs., IR2:61–88 (1966).
17. Palosaari, S. M. *Steady State Effective Thermal Conductivity of Wetted*

Closed Porous System, Ph.D. Thesis at Imp. College of Science and Tech., U. of London, pp. 1–224 (1972); see also Palosaari, S. M. and A. R. H. Cornish. *Acta Polytechnica Scandinavica.* Helsinki, Chapters 125, 126 and 128 (1972).

18. Crank, J. *The Mathematics of Diffusion.* Oxford:Clarendon Press (1975).
19. Kumaran, M. K. and G. P. Mitalas. "Analysis of Simultaneous Heat and Moisture Transport Through Glass Fibre Insulation," ASME/AIChE 1987 Nat. Heat Transfer Conf., Pittsburgh (Aug. 9–12, 1987).
20. Brandreth, D. A. *J. of Thermal Insulation,* 5:31–39 (July 1981).
21. Sparks, L. L. and J. M. Arvidson. *Journal of Thermal Insulation,* 8:198–231 (Jan. 1985). (Data taken from original report of NBS No. GRI-84/0086.)
22. Bigolaro, G., F. De Ponte and E. Fornasieri. "Thermal Conductivity of Polyurethane at Low Temperatures," manuscript from Padova University, pp. 1–9, published in *Proceedings of Int. Institute of Refrigeration,* Commission B1, Washington, D.C., pp. 14–17 (1976).

BIOGRAPHY

Mark Bomberg

Mark Bomberg, senior research officer at the National Research Council, is a member of Committees C-16 on Thermal Insulation and E-6 on Performance of Building Constructions. Bomberg was born and educated in Warsaw, Poland. He obtained an M.Sc. in civil engineering, and a D.Sc. at the Warsaw Institute of Technology. Between 1967 and 1975, Bomberg worked at the Division of Building Technology, Lund Institute of Technology. He then emigrated to Canada, joining the National Research Council of Canada in Saskatoon and later in Ottawa. He is responsible for the development of test methods for testing thermal insulation.